Eur. Phys. J. D **30**, 327–333 (2004)
DOI: 10.1140/epjd/e2004-00105-4

THE EUROPEAN PHYSICAL JOURNAL D

Electronic predissociation: a model study

M. Erdmann, S. Baumann, S. Gräfe, and V. Engel[a]

Institut für Physikalische Chemie, Universität Würzburg, Am Hubland, 97074 Würzburg, Germany

Received 18 February 2004 / Received in final form 10 June 2004
Published online 24 August 2004 –

Abstract. The combined electronic and nuclear motion during a predissociation process is studied in a model system. The latter consists of an electron and an ion which are allowed to move in one dimension and interact with each other and two fixed ions via screened Coulomb interactions. The fragmentation dynamics is illustrated in terms of the temporal changes of electronic and nuclear densities. In this way it is possible to reveal the influence of non–adiabatic coupling, not only on the nuclear wave–packet motion, but also on the transient electronic structure.

PACS. 31.50.Gh Surface crossings, non-adiabatic couplings – 31.70.Hq Time-dependent phenomena: excitation and relaxation processes, and reaction rates

1 Introduction

A famous example for the breakdown of the Born–Oppenheimer adiabatic approximation [1] is the electronic predissociation of molecules [2]. Conventionally, two theoretical frameworks are used to describe such a decay mechanism. Within the so–called diabatic picture [3] this process occurs when a bound (diabatic) potential energy curve V_n^d is intersected by another potential V_m^d, the latter being repulsive. Including off-diagonal potential elements leads to a coupling of the bound–state manifold to the continuum, so that the molecule decays into fragments. This effect manifests itself in the energy dependence of observables such as absorption spectra [4] or scattering cross sections [5,6] in the form of resonances. In the case of a small diabatic coupling (the 'diabatic limit'), the decay occurs with a long lifetime of the quasi–bound complex which, in turn, means that the resonances have a small spectral width. The adiabatic picture of a predissociation provides a different approach for a physical description. The adiabatic potential curves $V_n^a(R)$ are uniquely obtained from the solution of the stationary Schrödinger equation for fixed nuclear geometry R. In the case where non–adiabatic effects are large, an adiabatic curve exhibits an avoided crossing (diatomic molecule) [7] or a conical intersection (polyatomic molecule) [8] with the potential surface of another electronic state. The interaction is provided by kinetic coupling elements containing derivatives of the electronic wave function with respect to the nuclear coordinates. The case of a strong coupling, corresponding to a large probability to change the adiabatic electronic state, is identical to the case of a weak diabatic coupling which often leads to confusion if the couplings and the zeroth–order picture of the description are not accurately defined.

Within the adiabatic picture, the quantum mechanics of an electronic predissociation process is described most illustratively in terms of a multi–component nuclear wave–packet dynamics. As a textbook example one may regard the NaI molecule which was investigated by Zewail and co–workers using femtosecond time–resolved spectroscopy [9]. In this molecule, the electronic ground state exhibits an avoided crossing with an excited state. Upon femtosecond pulse–excitation from the ground to the excited state, a vibrational wave packet is prepared and moves outward until the crossing region is reached. Here, the packet splits into two parts: a first one remains in the upper state, performing a quasi–bound vibrational motion, whereas a second part crosses to the ground state, leading to fragmentation into Na and I atoms [10]. In the latter particular example, the nuclear dynamics is accompanied by a charge–transfer process which has been nicely illustrated by Grønager and Henriksen [11]. It is clear that, during an electronic predissociation, substantial changes of the electron density are to be expected. Unfortunately, a complete quantum description including both the nuclear and electronic degrees of freedom is — up to date — only possible within very limited models. For a review on different methods to approach the problem of combined electronic and nuclear motion, see e.g. reference [12].

One possibility to tackle the description of molecules beyond adiabatic approximations is that of reduced dimensionality. For example, Bandrauk and co–workers have studied laser-excitation processes for systems within a linear configuration [13–15]. In a recent study we have

[a] e-mail: voen@phys-chemie.uni-wuerzburg.de

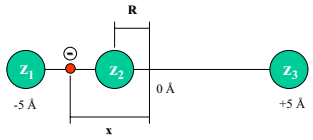

Fig. 1. Particle configuration of the model system. Two fixed ions with charges Z_1 and Z_3 are separated by a distance of 10 Å. An electron with coordinate x and an ion (Z_2) with coordinate R are allowed to move in one dimension.

treated a linear H_2 molecule interacting with strong laser fields [16]. Also, efforts have been undertaken to develop a two–component time–dependent density functional theory for the treatment of molecules in laser fields [17]. In the present paper we aim at the description of an electronic predissociation process employing a model which originates in the work of Shin and Metiu [18,19] and was investigated by us in terms of electronic-vibrational density dynamics [20] and its modification by the interaction with external fields [21]. The main purpose is to illustrate the nucleus mediated transient electronic structure during the molecular fragmentation. The model and its theoretical treatment is described in Section 2. In Section 3, various adiabatic potential curves and the corresponding electronic eigenfunctions are discussed. The quantum dynamics is described in Section 4 which also contains a short summary.

2 Theory and model

Following former work [18,19], we define a model including three ions and an electron arranged in one spatial dimension. Here, two ions (referred to as ion (1) and ion (3), in what follows) are separated by a fixed distance L, whereas the third ion (2) with coordinate R and the electron with coordinate x are allowed to move. The distances R, x refer to the origin of the coordinate system which is located in the middle between the ions (1) and (3). The linear particle configuration and the associated coordinates are illustrated in Figure 1.

The Hamiltonian of the system is (atomic units are employed):

$$H = -\frac{1}{2}\frac{\partial^2}{\partial x^2} - \frac{1}{2m}\frac{\partial^2}{\partial R^2} + V(x,R), \tag{1}$$

where the potential energy is parameterized in the form

$$\begin{aligned} V(x,R) = &\frac{Z_1 Z_2}{|L/2+R|} \\ &+ Z_2 Z_3 \frac{\mathrm{erf}(|L/2-R|/R_{23})}{|L/2-R|} - Z_1 \frac{\mathrm{erf}(|L/2+x|/R_{1e})}{|L/2+x|} \\ &- Z_2 \frac{\mathrm{erf}(|R-x|/R_{2e})}{|R-x|} - Z_3 \frac{\mathrm{erf}(|L/2-x|/R_{3e})}{|L/2-x|}. \end{aligned} \tag{2}$$

The repulsion of ions (1) and (3) is omitted since it represents an additive constant to the Hamiltonian (1). The first term in the expression for the potential describes the bare Coulomb repulsion of ions (1) and (2) whereas a screened Coulomb interaction between ions (2) and (3) is parameterized by an error function erf (second term). The same functional form is employed for the ion–electron attraction. The parameters entering into the Hamiltonian are the mass m, the nuclear charges $Z_n (n = 1-3)$, the distance L and the screening radii R_{23}, $R_{ne} (n = 1-3)$.

Fixing the nuclear coordinate R, adiabatic potential curves are calculated as the R–dependent eigenenergies of the electronic Schrödinger equation

$$\left\{ -\frac{1}{2}\frac{d^2}{dx^2} + V(x,R) \right\} \varphi_n(x,R) = V_n^a(R)\, \varphi_n(x,R), \tag{3}$$

where $\varphi_n(x,R)$ are the electronic eigenfunctions in the electronic state $|n\rangle$.

To characterize the dynamics in the system, we numerically integrate the time–dependent Schrödinger equation with the Hamiltonian (1) using a grid representation of the wave function $\psi(x,R,t)$ and the propagation method of Feit and Fleck [22]. From the time–dependent wave function we calculate the nuclear

$$\rho(R,t) = \int dx\, |\psi(x,R,t)|^2 \tag{4}$$

and electron density

$$\rho(x,t) = \int dR\, |\psi(x,R,t)|^2. \tag{5}$$

Furthermore, using the electronic basis functions as defined in equation (3), the nuclear densities within a particular electronic state $|n\rangle$ are obtained by projection:

$$\rho_n(R,t) = \left| \int dx\, \varphi_n(x,R)\, \psi(x,R,t) \right|^2. \tag{6}$$

3 Electronic structure

The functional form of the potential energy (Eq. (2)) allows to modify the particle interaction in a convenient way. We will now show that, using this parameterization, it is possible to generate adiabatic potential energy curves $V_n^a(R)$ for the nuclear motion describing various generic electronic structures which also occur in diatomic molecules. In order to restrict the parameter space the mass of the moving ion is fixed to the hydrogen mass and the stationary ions (1) and (3) are kept at a distance of $L = 10$ Å. The screening radii corresponding to the electron's interaction with the fixed ions were set to $R_{1e} = R_{3e} = 1.5$ Å. The charges will be allowed to assume also non–integer numbers, are thus no atomic charges and have to be interpreted as effective charges.

Figure 2 displays potential curves for the electronic ground ($|0\rangle$) and first excited state ($|1\rangle$), calculated for different parameters. The upper panel (a) contains the case where the ground–state potential exhibits a double-minimum structure and the first excited state is separated

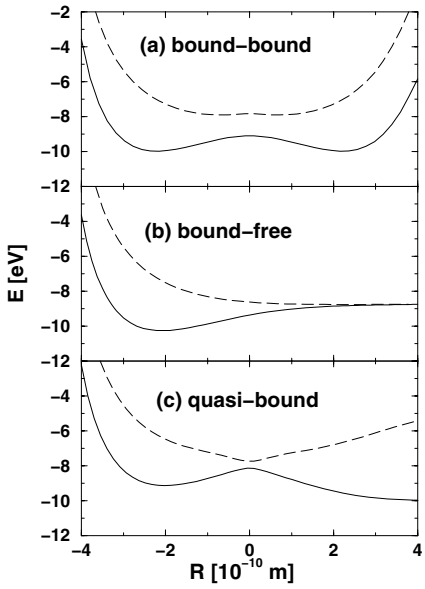

Fig. 2. Adiabatic potential energy curves for the electronic ground ($n = 0$) and first excited state ($n = 1$), calculated using different parameters entering into the interaction potential of the model system. Panel (a) shows the case of an electronic ground state having a double minimum potential and an energetically separated excited state ($Z_n = 1$, $R_{2e} = 1.5$ Å, $R_{23} = 1$ Å). The case of a bound ground and dissociative first excited state is illustrated in panel (b) ($Z_1 = Z_2 = 1$, $Z_3 = 0.001$, $R_{2e} = R_{23} = 1.5$ Å). Panel (c) contains curves where ground and excited state potentials exhibit an avoided crossing which is typical for a predissociation process ($Z_n = 1$, $R_{2e} = 1.75$ Å, $R_{23} = 2.3$ Å).

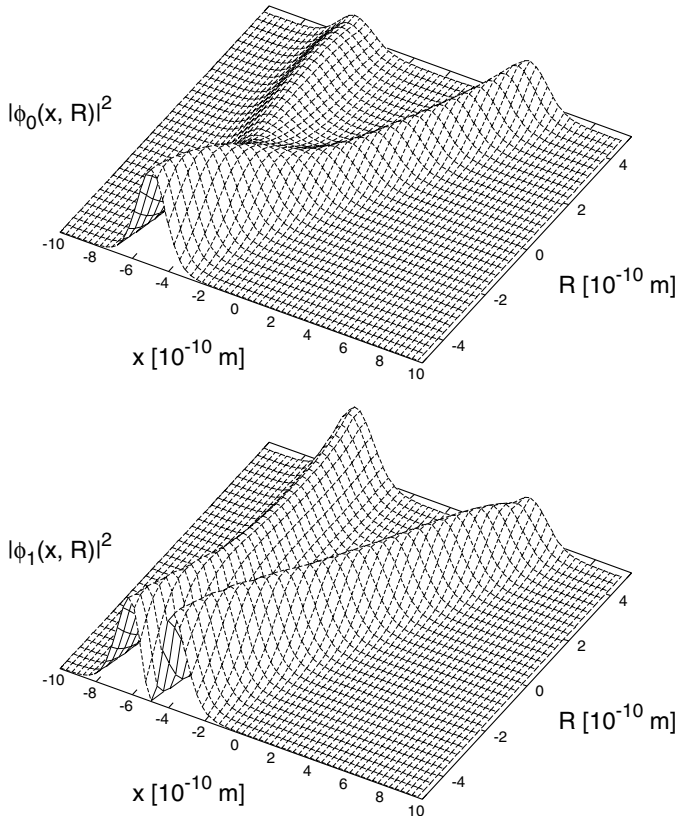

Fig. 3. Electronic probability densities $|\varphi_n(x, R)|^2$ for the case of a bound ground state ($n = 0$) and a dissociative excited state ($n = 1$), see Figure 2, panel (b).

by a larger gap of about 0.5 eV. In calculating the curves, all charges were set to $Z_n = 1$, the electron-nuclear interaction was determined with $R_{2e} = 1.5$ Å and the nuclear interaction of ions (2) and (3) contained the parameter $R_{23} = 1$ Å. The plot illustrates a situation where the adiabatic approximation between the nuclear and electronic degree-of-freedom applies. Such a case was investigated in detail before [18–21] and will thus not be discussed in what follows.

In order to encounter a situation characterized by a bound ground state and a dissociative excited state, the interaction of the ions (2) and (3) has to be diminished. Therefore we set $Z_1 = Z_2 = 1$ and $Z_3 = 0.001$, employing furthermore $R_{2e} = R_{23} = 1.5$ Å. Panel (b) of Figure 2 displays the calculated potential curves which are typical for a bound-to-free transition upon electronic excitation, as is already obtained in a simple LCAO-approach to e.g. the H_2^+ molecule using two basis functions.

Regarding panel (c) of Figure 2 ($Z_n = 1$, $R_{2e} = 1.75$ Å, $R_{23} = 2.3$ Å) we see that the lower and upper adiabatic potential curve exhibit an avoided crossing around $R = 0$ Å. Here the lower curve decreases in energy for distances R larger than $R = 0$, i.e. the system is not stable. This is the characteristic situation of an electronic predissociation where a (diabatic) 'quasi-bound' initial state decays via a coupling to a continuum.

Altogether, Figure 2 documents that within the parameterization of the potential energy (Eq. (2)), it is possible to generate adiabatic potential curves which are generic for ground and excited state configurations belonging to a bound-bound, bound-free and quasi-bound nuclear dynamics.

Let us next take a look at the electronic probability densities $|\varphi_n(x, R)|^2$ as calculated from the electronic Schrödinger equation (Eq. (3)). The absolute square of these functions for the bound–free case are displayed in Figure 3. The figure documents how the electronic properties of the system vary with the nuclear distance R. In order to investigate this behavior in more detail, we show cuts taken for selected values of R in Figure 4. The ground-state function for a value of $R = -2$ Å, which is close to the potential minimum of the lower adiabatic potential, resembles a Gaussian localized between the ions (1) and (2). Upon electronic excitation, the function remains in the same region of space, but naturally, acquires a node. For a nuclear position of $R = 0$ Å, the ground state density exhibits a double peak structure and in the excited state, the second maximum is shifted towards larger distances. These trends continue with increasing values of R and at $R = 4$ Å, where the potentials are almost degenerate, one obtains similar densities in ground and excited state.

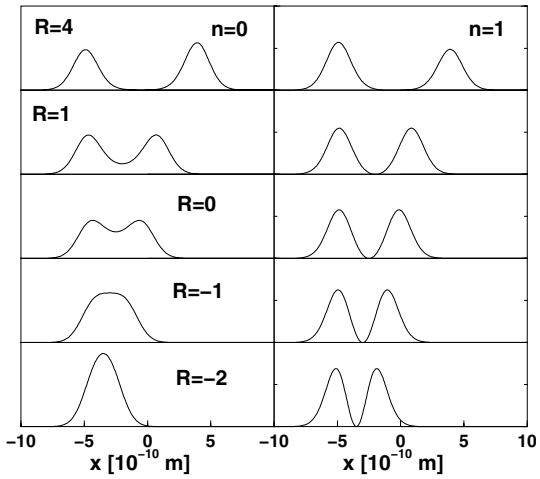

Fig. 4. Cuts through the densities $|\varphi_n(x,R)|^2$ displayed in Figure 3 (bound–free). The respective values of the nuclear coordinate R are given in Å.

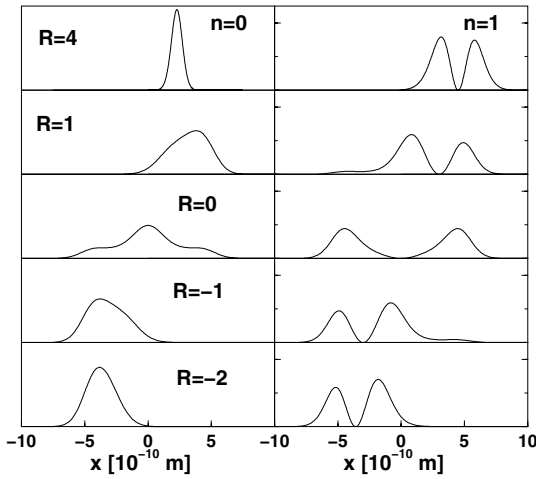

Fig. 6. Cuts through the densities $|\varphi_n(x,R)|^2$ displayed in Figure 5 (predissociation). The respective values of the nuclear coordinate R are given in Å.

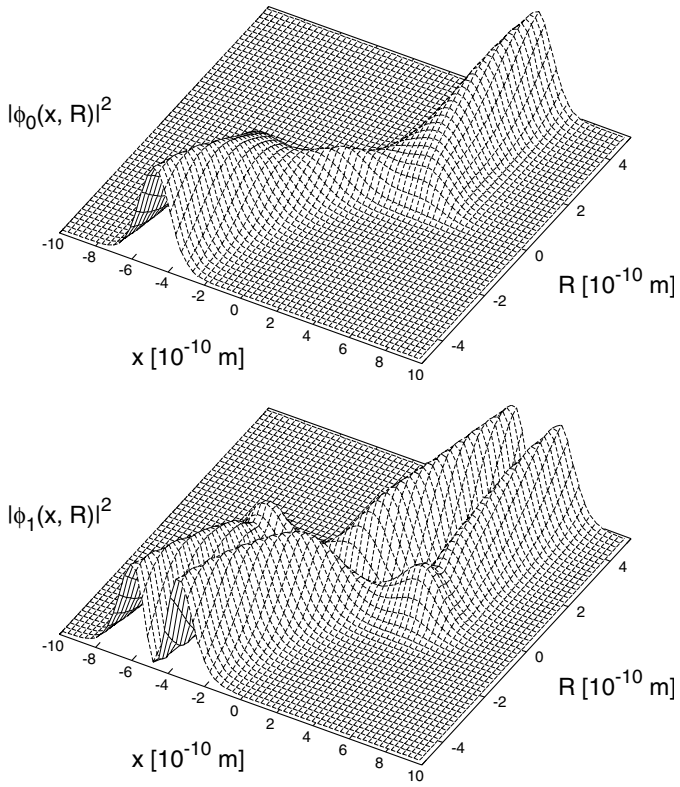

Fig. 5. Electronic probability densities $|\varphi_n(x,R)|^2$ in the predissociation case.

What happens in the case of the predissociation (see Fig. 2, panel (c)) is illustrated in Figure 5. The figure documents the influence of the non–adiabatic coupling: in the region around $R = 0$ Å, the character of the electronic wave functions changes strongly so that the derivatives of these functions with respect to the nuclear coordinate become large and the Born–Oppenheimer approximation breaks down. The electronic probability densities are shown for representative values of the nuclear coordinate R in Figure 6. At the minimum of the lower adiabatic curve ($R = -2$ Å), ground and excited state wave functions are similar to the bound-free case as discussed above: the electron is shared between ions (1) and (2). With increasing value of the nuclear coordinate R, the densities become more de-localized. If R assumes a value of 0 Å, that is, in the region where the avoided crossing of the curves appears, the ground state function exhibits three maxima indicating that all three ions participate in the bonding situation (three-center). In the excited state, the node of the wave function coincides with the location of ion (2) ($x = R = 0$ Å). At large R (here $R = 4$ Å), we find a similar situation as encountered for $R = -2$ Å but now the electronic wave functions are located between the ions (2) and (3).

4 Time–dependent densities

First we treat the direct dissociation process. Therefore the parameters were chosen as in the bound-free case leading to the potential curves displayed in Figure 2, panel (b). Here the initial state was a Gaussian

$$\psi(x,R,t=0) = e^{-\beta(R-R_0)^2}\ \varphi_n(x,R), \qquad (7)$$

with $\beta = 1.06$ Å^{-1} and $R_0 = -2.5$ Å times the electronic eigenfunctions with $n = 1$. The wave function at $t = 0$ can be imagined to result e.g. from a femtosecond excitation process originating in another electronic state (for example the ground state). A change of the center of the initial state does not change the dynamical picture as discussed below. The same applies to the width of the Gaussian. Insofar, the here presented case can be regarded as typical.

Starting in the repulsive excited state, the nuclear density (upper panel in Fig. 7) moves outward until it reaches the region where an optical potential was used in the calculation (at distances larger than $R = 4$ Å) to continuously remove the outgoing parts of the wave

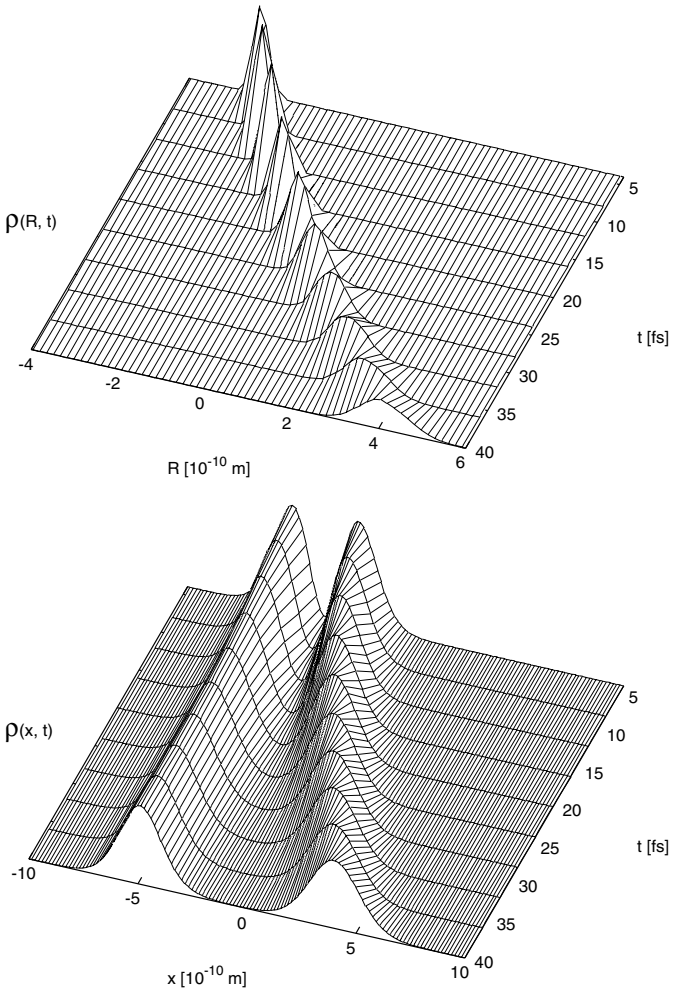

Fig. 7. Upper panel: nuclear density dynamics in the case of a direct dissociation. The lower panel displays the corresponding time–dependent electron densities.

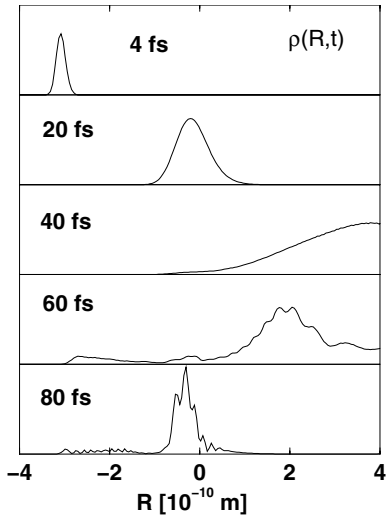

Fig. 8. Electronic predissociation: cuts of the nuclear density are shown at different time, as indicated.

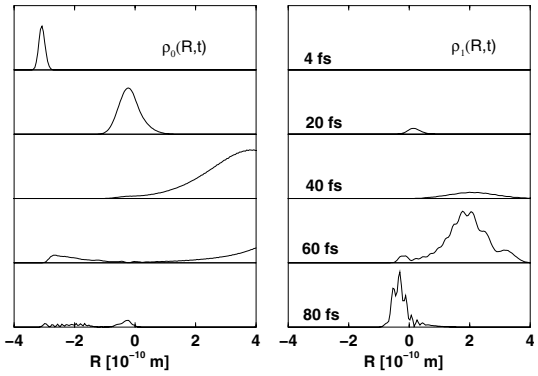

Fig. 9. The densities in the ground (left panels) and first excited (right panels) electronic state are displayed at different times (predissociation dynamics).

function [23,24]. The barrier-free fragmentation is accompanied by changes in the electronic density, as seen in the lower panel of the figure. The outward moving nucleus takes electron density away. However, with equal probability the electron remains localized close to the fixed ion (1).

In order to get some insight into the dynamics of the predissociation process we first analyze the nuclear dynamics. This is normally done by propagating wave packets on the diabatic potentials, including a potential coupling between the different states. Here we regard the coupled electronic-nuclear motion without involving the potentials for the nuclear motion. The initial wave function was of the form given in equation (7) with $\beta = 2.12$ Å^{-1}, $R_0 = -3.4$ Å and contained the electronic ground state wave function $\varphi_0(x, R)$. The initial state has an average energy which corresponds to the barrier height in the electronic ground state. A displacement of the function towards larger values of R results in a lower predissociation yield, i.e. the packet is trapped in the lower potential well — at least for the times regarded here. A displacement towards smaller distances puts us into the diabatic limit, where the non-adiabatic transition towards the higher electronic state occurs with unit probability. Therefore, the here discussed case represents an example where predissociation is effective on a short time-scale.

The time–evolution of the nuclear density (Eq. (4)) is shown in Figure 8. The initially localized Gaussian function moves towards larger distances and spreads substantially within the first 20 fs. The spreading proceeds and at 40 fs the density is almost totally localized at positive values of R. At later times, probability density moves inward, exhibiting a larger maximum around $R = 0$ Å (80 fs).

Regarding the total nuclear density it is not possible to decide which electronic states participate in the predissociation process. Therefore, we regard the projections $\rho_n(R, t)$, which are shown in Figure 9. For each time, the two densities are shown on the same scale but for different times, these scales are chosen differently. Since the initial wave packet is, by definition, a ground–state function, the projection $\rho_0(R, t = 0)$ is identical to the total density $\rho(R, t = 0)$, see Figure 8. As is seen in the total

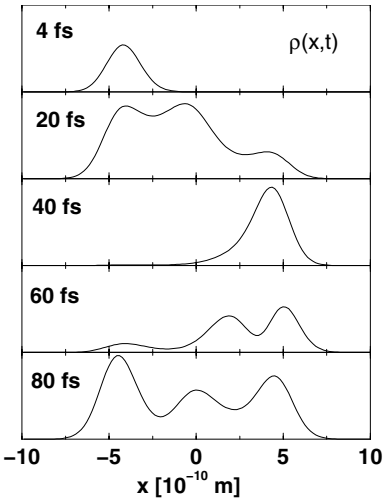

Fig. 10. Electron density dynamics during the predissociation process at selected times.

density, the function moves outward until it reaches the crossing region where the non-adiabatic coupling is effective (20 fs). Then, a bifurcation occurs so that partly a ground state dissociation, but also a transition to the excited state takes place (40 fs). At a time of 60 fs, the excited state density is reflected at the outer potential wall, thus exhibiting an oscillatory structure which is caused by the superposition of inward and outward moving components. There is, besides the dissociative part, another ground state component seen at negative distances, which corresponds to a flux reflected at the potential barrier. Finally, at a time of 80 fs, a re-population of the electronic ground state occurs, but most of the density remains in the excited state. The dynamics taking place at longer times proceeds accordingly and is not shown here.

The nuclear wave-packet dynamics for our model system is in accordance with the general quantum mechanical motion taking place on coupled potential energy surfaces. The advantage here is that we are in the position to simultaneously monitor changes of the electron density, i.e. we might answer our initially posed question of electronic structural changes during a predissociation process. Figure 10 contains the electron density for selected times, as indicated. At a time of 4 fs, where the nucleus is located at about $R = -3$ Å, the function is that of the electronic ground state (compare Fig. 6). A little later (20 fs), the mobile ion has reached the coupling region around $R = 0$ Å, but still most of the population is in the $n = 0$ state. Accordingly, the electron density is dominated by the features of the respective electronic wave function (Fig. 6, middle left panel). The same holds at a time of 40 fs where fragmentation has occurred with a relatively high probability. The electron density at 60 fs shows a different behavior. At positive values of the electron coordinate x, the nodal structure of the excited state electronic wave function becomes visible. Since the radial wave function has a component in the electronic ground state localized at negative values of R (see Fig. 9), the electron density exhibits another maximum around $x = -5$ Å which reflects the ground state electronic wave function. The lowest panel of Figure 10 shows a function with three maxima. Here the nuclear components in ground as well as excited state, are mainly localized in the region around $R = 0$ Å (see Fig. 9). By inspection of Figure 6 it is then clear, that the outer two maxima in $\rho(x,t)$ stem from the excited state whereas the middle maximum originates from a contribution from the ground electronic state. This of course means that the total wave function is strongly influenced by a non–adiabatic coupling.

To summarize, we have explored a simple model to describe a coupled electronic and nuclar motion. A particular form of parameterization of the particle interactions allows to create different bonding situations in the ground and an excited electronic state. These situations can be characterized by adiabatic potential curves with bound and dissociative character and also exhibiting an avoided crossing. The quantum dynamics for a direct dissociation involves a wave packet which directly moves into the exit channel. Thereby, it transports electron density in a smooth way. Regarding an electronic predissociation, we demonstrated how the character of the electron density changes during fragmentation. Here, the non–adiabatic coupling mixes properties of ground and excited state electronic wave function giving rise to a complicated transient electronic structure of the system.

The model which was used in the present work is very simple and uses a single electronic and nuclear degree of freedom and a linear configuration. Nevertheless, we think that it contains many essentials reflecting a realistic situation in small molecules. In the future extensions are possible, e.g. the inclusion of a second electron or nucleus could provide a deeper understanding of the dynamical features in systems composed of a few interacting particles.

This work was funded by the Deutsche Forschungsgemeinschaft within the Graduiertenkolleg 'Electron Density' and the NRC–Helmholtz (project: ADAM) program. We gratefully acknowledge support by the Fonds der Chemischen Industrie.

References

1. M. Born, K. Huang, *Theory of Crystal Lattices* (Oxford University Press, London, 1954)
2. G. Herzberg, *Spectra of Diatomic Molecules* (van Nostrand Reinhold, New York, 1950)
3. H. Köppel, W. Domcke, L.S. Cederbaum, Adv. Chem. Phys. **57**, 59 (1984)
4. R. Schinke, *Photodissociation Dynamics* (Cambridge University Press, Cambridge, 1993)
5. M.S. Child, *Molecular Collision Theory* (Dover Publications, Mineola, 1996)
6. B.H. Bransden, M.R.C. Mcdowell, *Charge Exchange and the Theory of Ion-Atom Collisions* (Clarendon Press, Oxford, 2003)
7. C.A. Mead, J. Chem. Phys. **70**, 2276 (1979)

8. *Conical Intersections: Electronic Structure, Dynamics and Spectroscopy*, edited by W. Domcke, D.R. Yarkony, H. Köppel (World Scientific, Singapore, 2004)
9. T.S. Rose, M.J. Rosker, A.H. Zewail, J. Chem. Phys. **91**, 7415 (1989)
10. V. Engel et al., Chem. Phys. Lett. **152**, 1 (1988)
11. M. Grønager, N.E. Henriksen, J. Chem. Phys. **109**, 4335 (1998)
12. E. Deumens, A. Diz, R. Longo, Y. Öhrn, Rev. Mod. Phys. **66**, 917 (1994)
13. H. Yu, T. Zuo, A.D. Bandrauk, Phys. Rev. A **54**, 3290 (1996)
14. S. Chelkowski, C. Foisy, A.D. Bandrauk, Phys. Rev. A **57**, 1176 (1996)
15. I. Kawata, H. Kono, A.D. Bandrauk, Phys. Rev. A **64**, 043411 (2001)
16. M. Lein, E. Gross, T. Kreibich, V. Engel, Phys. Rev. A **65**, 033403 (2002)
17. T. Kreibich, N.I. Gidopoulos, R. van Leeuwen, E. Gross, Prog. Theo. Chem. Phys. **14**, 69 (2003)
18. S. Shin, H. Metiu, J. Chem. Phys. **102**, 9285 (1995)
19. S. Shin, H. Metiu, J. Phys. Chem. **100**, 7867 (1996)
20. M. Erdmann, P. Marquetand, V. Engel, J. Chem. Phys. **119**, 672 (2003)
21. M. Erdmann, V. Engel, J. Chem. Phys. **120**, 158 (2004)
22. M.D. Feit, J.A. Fleck, A. Steiger, J. Comput. Phys. **47**, 412 (1982)
23. D. Neuhauser, M. Baer, J. Chem. Phys. **90**, 4351 (1989)
24. U.V. Riss, H.-D. Meyer, J. Chem. Phys. **105**, 1409 (1996)